Sensitivity of the $^{13}C(\alpha, n)^{16}O$ *S* factor to the uncertainty in the level parameters of the near-threshold state

R. J. deBoer,[1] C. R. Brune,[2] M. Febrarro,[3] J. Görres,[1] I. J. Thompson,[4] and M. Wiescher[1]

[1]*The Joint Institute for Nuclear Astrophysics, Department of Physics, Notre Dame, Indiana 46556, USA*

[2]*Edwards Accelerator Laboratory, Department of Physics and Astronomy, Ohio University, Athens, Ohio 45701, USA*

[3]*Oak Ridge National Laboratory, Oak Ridge, Tennessee 37830, USA*

[4]*Lawrence Livermore National Laboratory, Livermore, California 94550, USA*

(Received 20 January 2020; accepted 30 March 2020; published 20 April 2020)

The $^{13}C(\alpha, n)^{16}O$ reaction is the main source of neutrons for the *s* and *i* processes in asymptotic giant branch stars and carbon-enhanced metal-poor stars, respectively. The reaction rate over the relevant temperature range from 0.1 to 0.3 GK translates into a center-of-mass energy range of 150 to 540 keV. Current measurements extend down to 300 keV, still requiring an extrapolation of the cross section. At these low energies, the high-energy tail of a $1/2^+$ state near the reaction threshold makes a significant contribution to the cross section, but its amplitude is still highly uncertain. In this paper the uncertainties associated with the low-energy cross-section extrapolation are investigated, in particular the sensitivity to the energy, width, and Coulomb renormalized asymptotic normalization coefficient of the near-threshold resonance. Recently it has been suggested that the energy of the near-threshold level may have a large impact on the extrapolation, but this is not found to be the case compared with the other sources of uncertainty.

DOI: 10.1103/PhysRevC.101.045802

I. INTRODUCTION

The $^{13}C(\alpha, n)^{17}O$ reaction has been identified as the critical neutron source for the *s* process in low-mass asymptotic giant branch (AGB) stars [1] and the *i* process in carbon-enhanced metal-poor (CEMP) stars [2]. The *s* process in the helium-burning shell of AGB stars relies on an appreciable amount of ^{12}C being produced by the triple-alpha-process. Convective mixing of hydrogen into the shell triggers the reaction sequence $^{12}C(p, \gamma)^{13}N(\beta^+\nu)^{13}C$, and the amount of mixed-in hydrogen determines the intensity of the neutron flux. The actual process is not fully understood, but the proton infusion must be weak and well localized so that the $^{13}C(\alpha, n)^{16}O$ reaction dominates over the $^{13}C(p, \gamma)^{14}N$ reaction, which would otherwise trigger a CNO cycle. The conditions must be such that a proton-induced reaction is negligible. This requires a reduction of the $^{13}C(p, \gamma)^{14}N$ reaction by as much as eight orders of magnitude through hydrogen fuel removal or rapid temperature increase, as Fig. 1 indicates. It is an environmentally sensitive process [3], a balance between temperature and proton infusion, which needs sophisticated dynamic model treatment in order to evaluate its full impact [4].

The *i* process considers the special case of a deep convective environment in the helium burning zone in which the freshly produced ^{13}N is rapidly mixed to its hot bottom within a timescale comparable with the decay time of the nucleus ($\approx$10 minutes). The $^{13}C(\alpha, n)^{16}O$ reaction ignites at a much higher temperature, providing a much higher neutron flux of up to 10^{16} neutrons/cm^3 [2]. This process takes place in massive AGB stars and the characteristic abundance distribution is observed in early stars, so-called CEMP stars [4].

Reliable predictions of the efficiency of the $^{13}C(\alpha, n)^{16}O$ neutron source in an often highly dynamic environment of hydrogen ingestion into a carbon pocket coupled to a potentially deep convective helium burning shell in the *s* and even more so the *i* process requires a solid understanding of the reaction cross section at the associated Gamow energies ($0.1 < T < 0.3$ GK) of about $E_{\text{c.m.}} = 150$ to 300 keV and 200 to 540 keV, respectively. There have been a number of successful attempts to push the direct measurement of the reaction towards lower energies [7–13]. The *S*-factor data of the recent lowest-energy measurements [8,9] are consistent with an upswing towards lower energies, but the uncertainties on these low-energy data are quite significant. If confirmed in present underground experiments, this upswing would likely correspond to the tail of a previously observed broad near-threshold resonance that corresponds to the $J^\pi = 1/2^+$ level in ^{17}O at $E_x = 6.356(8)$ MeV [14], where the α-particle separation energy in ^{17}O (S_α) is 6.358 69 MeV [15,16].

This case of a near-threshold cluster resonance in the $^{13}C(\alpha, n)^{16}O$ reaction is an example of the impact of cluster configurations in nuclear astrophysics [17]. The existence of such cluster configurations near thresholds have been observed in many cases and are explained phenomenologically in the framework of the IKEDA rule [18]. For the case of the $^{13}C(\alpha, n)^{16}O$ reaction, Descouvemont [19] was the first to make a theoretical prediction of the level structure by using a microscopic generator-coordinate method (GCM). Recently, additional theoretical work has explained the appearance of such structures in close vicinity to threshold as a consequence

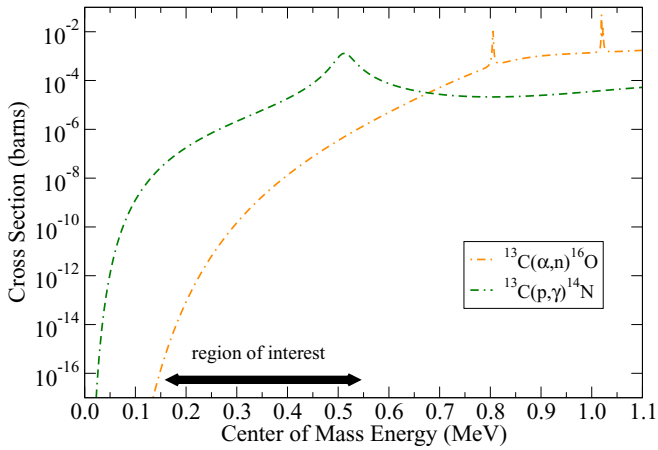

FIG. 1. Comparison of *R*-matrix evaluations for the $^{13}\mathrm{C}(\alpha, n)\,^{16}\mathrm{O}$ [5] and $^{13}\mathrm{C}(p, \gamma)\,^{13}\mathrm{N}$ reactions [6]. The arrow represents the energy region of interest for the *s* and *i* processes.

of an openness of the nuclear many-body system, which leads to the collectivization of shell-model (SM) states into cluster configurations [20]. This model demonstrates that the cluster configurations emerge fairly independent of the structure of the respective compound nucleus. This approach, the shell-model embedded in the continuum (SMEC), provides a unified description of structure and reactions with up to two nucleons in the scattering continuum using realistic SM interactions. This theory has been successfully applied to cases such as the cluster states facilitating the triple-alpha process [21].

Asymptotic normalization coefficients [22] C are often used to characterize the strength of bound states and have largely taken the place of spectroscopic factors in recent years [23,24]. The main advantage of their use is a reduced dependence on the properties of the nuclear potential used to extract them from transfer reaction data [25]. The value of C corresponds to the amplitude of the bound-state wave function, which is a function of the exponentially decaying Whittaker function. Deriving C in the framework of *R*-matrix theory [26], the contribution of the bound state to the reaction cross section can be calculated [27]. One complication is that, for levels that are very close to threshold, C becomes a very large number. Therefore, the Coulomb-renormalized asymptotic normalization coefficient was introduced to largely remove this dependence [28]. This is the situation for the $^{13}\mathrm{C}(\alpha, n)\,^{16}\mathrm{O}$ reaction where a $1/2^+$ state sits very close to the α-separation energy and, within the uncertainty of the compilation [14], may be either bound or unbound.

While recent direct measurements of the $^{13}\mathrm{C}(\alpha, n)\,^{16}\mathrm{O}$ reaction have already pushed into the astrophysical region of interest, an extrapolation is still required to reach the lowest energies. At these low energies it is expected that the near-threshold state will have a significant impact. Therefore it is useful to understand the impact of the uncertainties of the different level parameters that are used to characterize the cross-section contribution from this near-threshold level. In particular, these are the level energy, the neutron partial width Γ_n, and, if it is a bound state, the square of the Coulomb-renormalized asymptotic normalization coefficient $\widetilde{C}^2$ [28]. If instead the state is α-particle unbound, an α-particle partial width (Γ_α) is used in place of $\widetilde{C}^2$. All of the these parameters have some associated uncertainty, and a major part of this work will be reviewing which of them dominate the uncertainty budget in the *R*-matrix calculation of the *S* factor.

In particular, it has recently been noted by Keeley *et al.* [29] that the uncertainty in the energy of the near-threshold state may lead to a significant uncertainty in the calculation of $\widetilde{C}^2$ from the distorted wave Born approximation (DWBA) analysis used to fit the transfer reaction data. Furthermore, there is a rather significant spread in the reported values of Γ_n of this state [9,30–32] and it is unclear how much this effects the extrapolation. Up until recently there was an apparent discrepancy between the $\widetilde{C}^2$ values determined through sub-Coulomb [33] transfer and through the Trojan horse method (THM) [31]. However, recently the THM data have been re-analyzed, given a new measurement of the energy and width of the near-threshold state [32], and it has been shown that the two measurement techniques yield consistent results [34,35]. Here we examine these sources of uncertainty and how they propagate to the uncertainty in the reaction rate in order to clarify which make the largest contributions and what the goals should be for future experimental measurements.

In Sec. II some general details and assumptions of the *R*-matrix calculations are given. This is followed by a detailed description of the steps needed to calculate the *S* factor from $\widetilde{C}^2$ in Secs. III and IV. The uncertainty in the *S* factor is then investigated considering the uncertainties in $\widetilde{C}^2$ in Sec. V and calculations are made for several past values of $\widetilde{C}^2$ in Sec. VI. The uncertainty from variations in the width is then presented in Sec. VII, from the overall normalization in the $^{13}\mathrm{C}(\alpha, n)\,^{16}\mathrm{O}$ reaction data in Sec. VIII, and then the most significant contributions are summarized in Sec. IX. The uncertainties are then propagated to the reaction rate in Sec. X. A final summary and discussion of the focus of future experiments is given in Sec. XI.

II. NOTES ON THE *R*-MATRIX CALCULATIONS

In this work the astrophysical *S* factor is calculated by using phenomenological *R* matrix [26] using the code AZURE2 [36,37]. Different sets of level parameters are investigated for the near-threshold state in $^{17}\mathrm{O}$ in order to test the sensitivity of the low-energy extrapolation to the associated uncertainties and discrepancies. No *R*-matrix fits are performed, because a proper refitting of the data would entail a new global analysis of many different data sets, including those from the $^{13}\mathrm{C}(\alpha, n)\,^{16}\mathrm{O}$ reaction as well as data from the $^{13}\mathrm{C}(\alpha, \alpha)\,^{13}\mathrm{C}$ reaction and $^{16}\mathrm{O}+n$ reactions. Instead, the best-fit parameters of a recent global fit of Leal *et al.* [5] are used. Only the energy, Γ_n and $\widetilde{C}^2$ (or Γ_α) of the near-threshold state are varied. For all of the comparison calculations, the data of Drotleff *et al.* [8], Heil *et al.* [9], and Harissopulos *et al.* [10] are used as representative data sets to compare the calculations with experimental results. In examining the comparisons between these data sets and the fit of Leal *et al.* [5], the fit does not match the data well over some regions. This is because there

is tension between the data sets shown and the many other data that were included in the global fitting that are not shown.

For all calculations, a channel radius of $a_c = 6.684$ fm is used for all α-particle channels and $a_c = 4.15$ fm is used for all neutron channels. The calculations are also done in the Brune parametrization [38], allowing for the direct use of observable level energies, widths, and reduced-width amplitudes. This also eliminates the need for boundary conditions. To aid in future work the AZURE2 input file used for these calculations is provided in the Supplemental Material [39].

III. CONVERSION OF $\widetilde{C}^2$ TO C

As a first step, the conversion from $\widetilde{C}^2$ to C is made. The practical reason for this initial conversion is that the AZURE2 [36,37] R-matrix code takes C instead of $\widetilde{C}^2$ as an input parameter. The conversion also points out many of the physical quantities, which are usually treated as constants in the calculations, that also have uncertainties that may need to be investigated. This section follows closely the calculations made in Keeley *et al.* [29] and Mukhamedzhanov *et al.* [34], but some additional points of clarification are made.

As discussed in Sec. I, the $1/2^+$ state is very close to threshold, implying that C will be a very large number due to the very small value of the Whittaker function close to the threshold energy. Therefore $\widetilde{C}^2$ has been adopted by all recent transfer studies to give a more convenient numerical representation [28]

$$\widetilde{C} = \frac{\ell!}{\Gamma(\ell+1+\eta)} C, \tag{1}$$

where ℓ is the relative angular momentum of entrance channel particles, η is the Sommerfeld parameter ($Z_a Z_A e^2 \mu_{aA}/k_{aA}$), k_{aA} is the wave number ($\sqrt{2\mu_{aA}\epsilon}$), Z_a and Z_A are the atomic numbers of the entrance channel particles, μ is the reduced mass [$m_a m_A/(m_a+m_A)$], m_a and m_A are the masses of the entrance channel particles, ϵ is the binding energy ($S_\alpha - E_{\text{c.m.}}$), and Γ is the gamma function.

Initially, the value of $\widetilde{C}^2$ from Avila *et al.* [33] will be used for the calculations. First the simple transformation is made from $\widetilde{C}^2 = 3.6(7)$ fm^{-1} to $\widetilde{C} = 1.9(2)$ fm$^{-1/2}$. Next, to calculate C from $\widetilde{C}$, the binding energy η, masses, and atomic numbers are needed. For the $\alpha + {}^{13}$C system, $Z_a = 2$, $Z_A = 6$, $m_a = 4.002\,603\,254\,13(6)$ u, and $m_A = 13.003\,354\,835\,21(23)$ u [15,16]. A very important part of this procedure is to note that in Avila *et al.* [33], a value of $E_x = 6.356$ MeV was used for the level energy of the DWBA analysis. The uncertainty in the level energy is unimportant at this point; it is, however, very important to note that the same energy must be used that was applied in the DWBA analysis of the transfer data, as this was the energy where the Whittaker function was evaluated in that analysis. To convert to a binding energy the α-separation energy must also be specified ($S_\alpha = 6.358\,69$ MeV [15,16]). Since the masses of ^{4}He, ^{13}C, and ^{17}O [$m_{^{17}\text{O}} = 16.999\,131\,756\,64(70)$ u] are known to high precision, the uncertainty in the masses and therefore the separation energy do not make a significant contribution to the uncertainty in this case and thus $\epsilon = 2.69$ keV, leading to a value of $\eta = 63.7462$. For a $J^\pi = 1/2^+$ level in the ^{17}O system, a $^4\text{He} + {}^{13}\text{C}$ partition can only be populated with a relative orbital angular momentum of $\ell = 1$ [channel spin (s) = 1/2]. Inserting into Eq. (1), $C = 5.44(54) \times 10^{90}$ fm$^{-1/2}$.

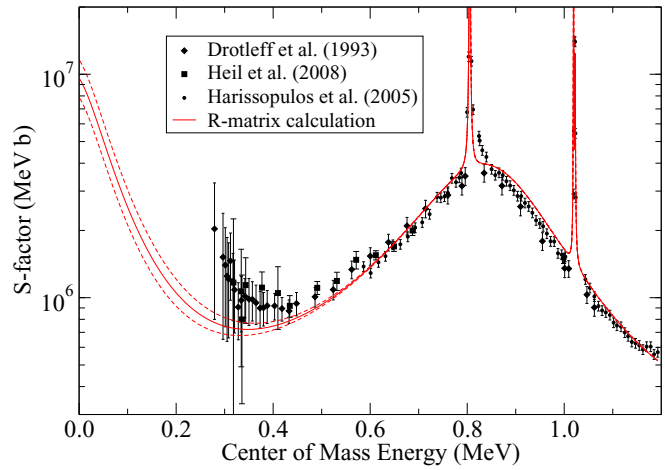

FIG. 2. Astrophysical S factor calculated by using C from Avila *et al.* [33] and the R-matrix level parameters from Leal *et al.* [5] (red solid line). The calculation is compared with the data of Drotleff *et al.* [8], Heil *et al.* [9], and Harissopulos *et al.* [10].

IV. INITIAL S FACTOR AND REDUCED-WIDTH AMPLITUDE CALCULATION

Applying the level energy adopted for the DWBA analysis, C, and $\Gamma_n = \Gamma = 145$ keV [5] to the R-matrix calculation discussed in Sec. II, the astrophysical S factor can be calculated as shown in Fig. 2. Now that the central value for the S factor has been calculated, the uncertainties are propagated from the uncertainty in the energy of the level and the uncertainty in $\widetilde{C}^2$. This is where the results of Ref. Keeley *et al.* [29] need to be considered carefully. The goal is to test if the variation observed by Keeley *et al.* [29] represents some other difference in the DWBA analysis or if this variation is simply an artifact of the rapid change in the Whittaker function near the threshold. If the variation is only due to the Whittaker function, this is not a real uncertainty, as will become clear when the calculations are carried through the R-matrix analysis.

Moving back to the R-matrix calculations, since a variation in the energy of the level will be made very close to threshold, it is more practical to deal with the R-matrix reduced-width amplitude $\widetilde{\gamma}_{\lambda c}$, because it is an energy-independent quantity. The downside is that this parameter is dependent on the choice of channel radius and R-matrix parametrization. Here λ and c are the level and channel indexes as adopted by Lane and Thomas [26]. By using the reduced-width amplitude, the energy dependence on the Whittaker function is removed. Furthermore, this provides a natural method for moving this state from a bound to unbound energy. This is the same procedure that was applied by Mukhamedzhanov *et al.* [34] for similar calculations.

At the excitation energy used by Avila *et al.* [33] of $E_x = 6.356$ MeV, the reduced-width amplitude is calculated from C

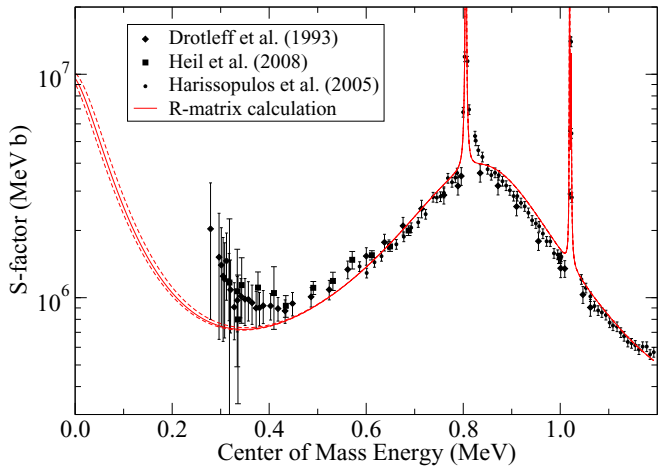

FIG. 3. Same as Fig. 2, but the uncertainty reflects the uncertainty in the level energy when $\tilde{\gamma}_\alpha$ is held constant.

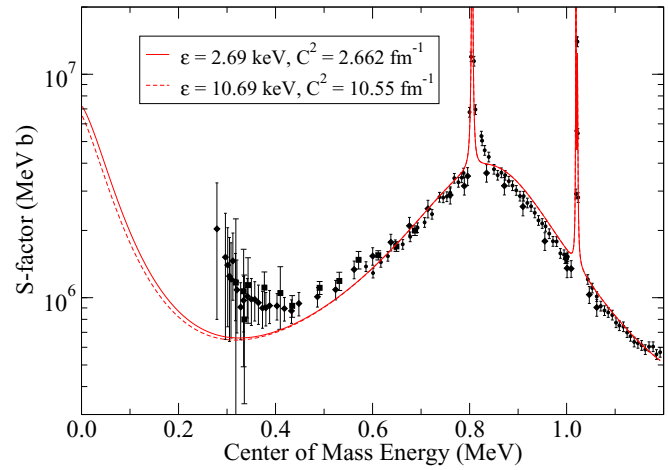

FIG. 4. Same as Fig. 2, but the calculations now use the values for C calculated from $\widetilde{C}^2$ from Keeley *et al.* [29]. See text for details.

with the AZURE2 code using [36,37,40]

$$C_{\lambda c} = \frac{(2\mu_\alpha a_c)^{1/2}}{\hbar W_c(a_c)} \left(\frac{\tilde{\gamma}_{\lambda c}}{\left[1 + \sum_{c'} \tilde{\gamma}^2_{\lambda c'} (dS_{c'}/dE)(\tilde{E}_\lambda)\right]^{1/2}} \right), \quad (2)$$

where $W_c(a_c)$ is the exponentially decaying Whittaker function evaluated at the channel radius a_c and $\tilde{\gamma}_{\lambda c}$ is the on-resonance (or Brune parametrization [38]) reduced-width amplitude. With the above parameters, $\tilde{\gamma}_\alpha = 0.199$ MeV$^{1/2}$. Note that, since the near-threshold state is the only level being referenced and there is only one R-matrix channel in the α-particle partition, the indexing has been simplified.

V. *S*-FACTOR UNCERTAINTY FROM *C*

As a first step, only the uncertainty in $C = 5.44(54) \times 10^{90}$ fm$^{-1/2}$ of Avila *et al.* [33] will be considered. This gives the uncertainty range shown in Fig. 2 and establishes a baseline uncertainty range that can be compared with contributions from other sources. This uncertainty is taken to be independent of the level energy.

Now the contribution from the uncertainty in the level energy of the $1/2^+$ state will be investigated. As in Keeley *et al.* [29], the value and uncertainty of the level energy will be taken from the compilation [14] as 6.356(8) MeV. The uncertainty considering the more precise value of the level energy reported recently by Faestermann *et al.* [32] will be discussed later.

First the lower bound of the uncertainty will be investigated at $E_x = 6.348$ MeV ($\epsilon = 10.69$ keV) and holding $\tilde{\gamma}_\alpha = 0.199$ MeV$^{1/2}$ constant. For comparison, this gives $C = 3.08 \times 10^{37}$ and it follows that $\widetilde{C}^2 = 11.8$ fm^{-1}. As expected, changing the energy of the bound state results in a large increase of 8.2 fm^{-1} in $\widetilde{C}^2$ from the initial value of 3.6 fm^{-1}. The resulting lower bound S factor is shown by the lower red dashed line in Fig. 3. The result is quite close to the S factor that was calculated at $E_x = 6.356$ MeV, only 5% lower at zero energy, and is small compared with the 20% uncertainty in the S factor resulting from the quoted uncertainty in $\widetilde{C}^2$ from Avila *et al.* [33].

This can be compared with the calculations of Keeley *et al.* [29], but it should be noted that the comparison cannot be made directly since some different parameters were used by Keeley *et al.* [29] and Avila *et al.* [33] that resulted in different values for $\widetilde{C}^2$ given in Fig. 1 of Keeley *et al.* [29]. For each of the $\widetilde{C}^2$ calculated by Keeley *et al.* [29] at different energies in Fig. 1 of their work, the S factor has been calculated. It was found that there is a dependence on the energy that seems to be beyond just that resulting from the Whittaker function. The difference grows as the difference in energy becomes larger. For the base value of $E_x = 6.356$ MeV ($\eta = 2.69$ keV), Keeley *et al.* [29] obtained $\widetilde{C}^2 = 2.662$ fm^{-1}, which results in $C = 4.69 \times 10^{90}$ fm$^{-1/2}$. This can then be compared with the value at their maximum energy difference of $E_x = 6.348$ MeV ($\eta = 10.69$ keV) where $\widetilde{C}^2 = 10.6$ fm^{-1}, which corresponds to $C = 2.61 \times 10^{37}$ fm$^{-1/2}$. This maximum deviation in the S factors is shown in Fig. 4 and corresponds to a maximum difference in the two S- actors of ≈10%.

Second, the upper value of $E_x = 6.364$ MeV is investigated. With the R-matrix reduced-width amplitude calculated, the calculation is straightforward. Now that the level is above the threshold ($E_{\text{c.m.}} = 5.31$ keV), the α-particle partial width was then calculated by using AZURE2 [36,37]:

$$\tilde{\Gamma}_{\lambda c} = \frac{2P_c \tilde{\gamma}^2_c}{1 + \sum_{c'} \tilde{\gamma}^2_{\lambda c'} \frac{dS_{c'}}{dE}(\tilde{E}_\lambda)}, \quad (3)$$

where $\tilde{\Gamma}_{\lambda c}$ is the partial width of level λ, P_c is the penetrability and S_c is the shift function. This gives a value of $\Gamma_\alpha = 2.54 \times 10^{-112}$ eV. The resulting S factor is shown as the upper red dashed line in Fig. 3 and deviates ≈5% from the baseline calculation. A summary of the different energy-related parameters for the near-threshold state is given in Table I.

VI. *S*-FACTOR CALCULATIONS FOR OTHER RECENT DETERMINATIONS OF $\widetilde{C}^2$

Calculations of the S factors and their corresponding uncertainties resulting from the uncertainty in $\widetilde{C}^2$, see Table II, are given for other past measurements in Figs. 5 and 6.

TABLE I. Summary of quantities calculated in gauging the uncertainty on the S-factor extrapolation of the $^{13}C(\alpha, n)^{16}O$ reaction due to the uncertainty in the energy of the near-threshold state. The calculations are made with $\widetilde{C} = 1.9$ fm$^{-1/2}$ and $\tilde{\gamma}_\alpha = 0.199$ MeV$^{1/2}$ ($a_c = 6.684$ fm).

E_x (MeV)	ϵ (keV)	η	C (fm$^{-1/2}$) or Γ_α (eV)
6.356	2.69	63.7462	$5.44(54) \times 10^{90}$
6.348	10.69	31.9773	3.08×10^{37}
6.364	−-5.31		2.54×10^{-112}

For the THM measurements, there have been substantial revisions [31,34,35] since the initial publication of La Cognata *et al.* [41]. As of Trippella and La Cognata [35] and Mukhamedzhanov *et al.* [34], the S factor calculated from the THM measurements is now similar to that calculated with $\widetilde{C}^2$ of Avila *et al.* [33]. However, because it will be utilized later for the uncertainty analysis, the S factor resulting from the $\widetilde{C}^2$ of La Cognata *et al.* [31] is calculated as shown in Fig. 5.

Three different transfer reactions have now been used to determine $\widetilde{C}^2$ for the near-threshold state. Avila *et al.* [33] has used $^{13}C(^6Li, d)^{17}O$, Pellegriti *et al.* [43] $^{13}C(^7Li, t)^{17}O$ and Guo *et al.* [44] and Mezhevych *et al.* [42] $^{13}C(^{11}B, ^7Li)^{17}O$.

VII. S-FACTOR UNCERTAINTY FROM NEUTRON WIDTH

There have also been rather discrepant values reported for Γ_n of the near-threshold state. If the state is bound, there are no other reaction channels open at this energy and the total width Γ is effectively equal to Γ_n. Even if unbound, Γ_α will be very small compared with Γ_n, as demonstrated in Sec. V. Obtaining accurate and precise values for the neutron width has proven to be quite challenging. At first this may be quite surprising because the near-threshold level produces a very distinguishable dip in the total neutron cross section, $^{16}O(n, \text{total})$, as observed in several measurements [45–48]. From these high-precision measurements it would seem that the width could also be obtained to high precision. However, the analysis is made more complicated that it might appear by the interference of other levels. For this reason, different

TABLE II. Summary of experimental determinations of $\widetilde{C}^2$ and the corresponding uncertainty when it is propagated to the low-energy S factor of the $^{13}C(\alpha, n)^{16}O$ reaction. The uncertainty stemming from the refitting of the data at different resonance energies is about 10% based on the consistency of $\widetilde{C}^2$ values calculated by Keeley *et al.* [29].

Ref.	$\widetilde{C}^2$ (fm^{-1})	% unc. in S
Pellegriti *et al.* [43]	4.5(22)	50
La Cognata *et al.* [31][a]	$7.7 \pm 0.3_{\text{stat}}{}^{+1.6}_{-1.5\text{norm}}$	20
Guo *et al.* [44]	4.0(10)	25
Avila *et al.* [33]	3.6(7)	20
Mezhevych *et al.* [42]	5.1(15) or 4.5(14)	30
Uncertainty in DWBA fitting [29]		10

[a]Re-evaluated in Trippella and La Cognata [35].

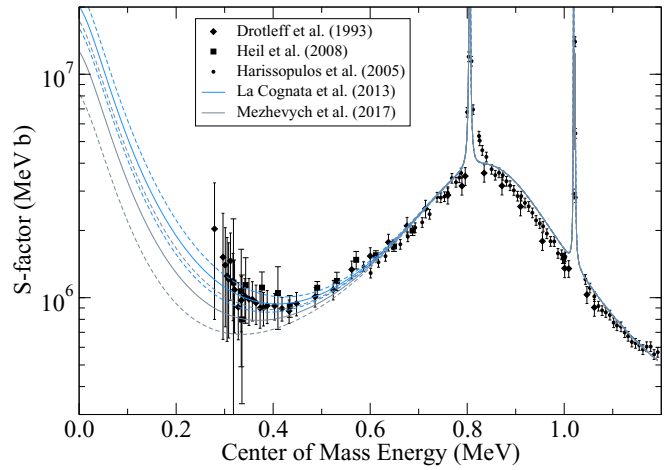

FIG. 5. Same as Fig. 2, but the calculations now reflect the $\widetilde{C}^2$ and their uncertainties from La Cognata *et al.* [31] and Mezhevych *et al.* [42].

phenomenological R-matrix fits have obtained different values for Γ_n even when much of the same data have been utilized [5,9,30]. The compilation [14] lists a value of $\Gamma_n = 124(12)$ keV.

To estimate the level of uncertainty in the S factor stemming from the uncertainty in Γ_n of the near-threshold state, calculations have been made for recently determined values of Γ_n [5,30,32] using the $\widetilde{C}^2$ of Avila *et al.* [33] and Γ_n from Leal *et al.* [5] for a baseline S-factor calculation as shown in Fig. 7. The low value of $\Gamma_n = 107$ keV from La Cognata *et al.* [31] has now been revised by Trippella and La Cognata [35] where the $\Gamma_n = 136$ keV from Faestermann *et al.* [32] is adopted. Therefore, this value can likely be discounted. The next lowest value is that of the compilation at $\Gamma_n = 124$ keV, which results in a maximum deviation in the S factor of ≈5% as shown in Fig. 7. For the high value, Sayer *et al.* [30] reports the largest value of $\Gamma_n = 162$ keV, which results in a difference in the S-factor over the region of interest of ≈5%. Figure 7 shows that despite this range of 55 keV difference in width,

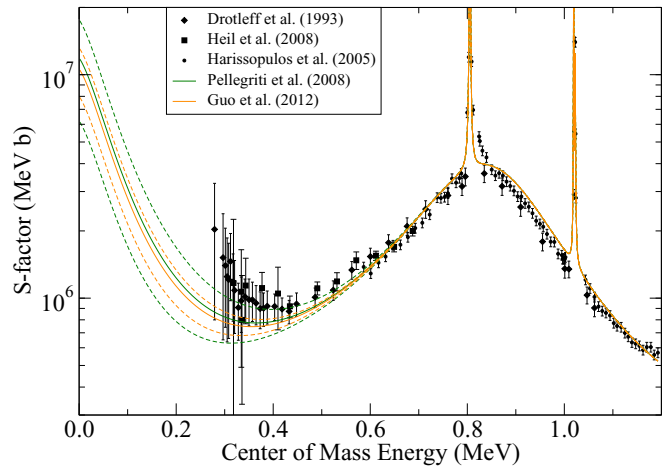

FIG. 6. Same as Fig. 2, but the calculations now reflect the $\widetilde{C}^2$ and their uncertainties from Pellegriti *et al.* [43] and Guo *et al.* [44].

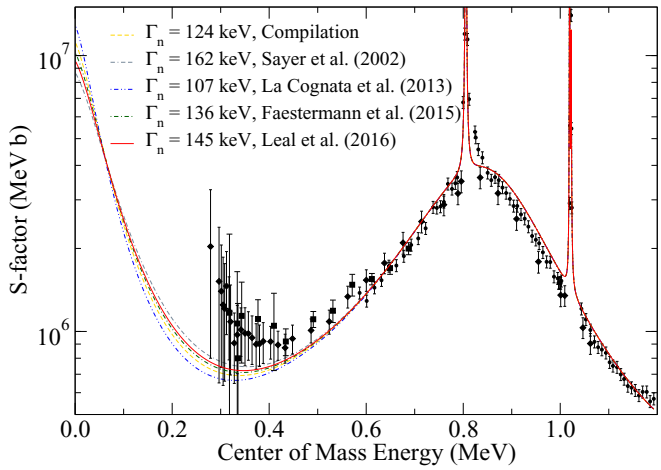

FIG. 7. Variation in the extrapolation of the low-energy S factor from different widths of the near-threshold state previously reported in the literature (solid lines) [5,14,30–32]. The S factor calculated with $\widetilde{C}^2$ from Avila *et al.* [33] and Γ_n from Leal *et al.* [5] is used as the reference calculation (red line). The data shown are the same as those in Fig. 2.

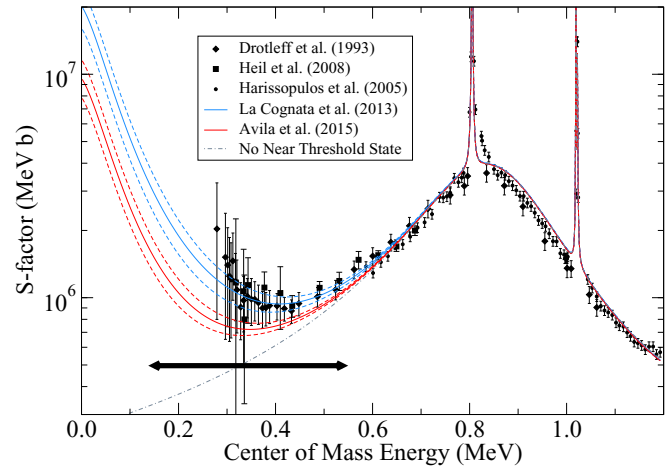

FIG. 8. S factors (solid lines) and their corresponding range of uncertainty (bounded by the dashed lines) for the $^{13}C(\alpha,n)^{16}O$ reaction using the $\widetilde{C}^2$ of La Cognata *et al.* [31] (blue) and Avila *et al.* [33] (red). The S factor with no near-threshold state contribution is shown by the gray dashed-dotted line. The black arrow indicates the energy range of astrophysical interest.

the extrapolated S factor is still almost completely within the range of the uncertainty from $\widetilde{C}^2$ of Avila *et al.* [33].

VIII. UNCERTAINTY FROM REACTION DATA

So far only uncertainties in the level parameters of the near-threshold state have been investigated, but these uncertainties need to be compared with the uncertainties on the reaction data itself in order to arrive at a more complete picture. There is a large inconsistency in the absolute cross section determined from different measurements, which has been a longstanding issue that has implications to the wider nuclear data community [49,50]. The uncertainty is reflected in the large difference in the evaluated cross section of the $^{16}O(n,\alpha)^{13}C$ reaction between ENDF/B-VII.1 [51] and ENDF/B-VIII.0 [49] of 32%. This uncertainty is primarily the result of differences in the absolute normalization of the cross-section measurements of Bair and Haas [52] and Harissopulos *et al.* [10], as discussed by Chadwick *et al.* [50].

Furthermore, as has been shown above, while the THM data and $\widetilde{C}^2$ values from the sub-Coulomb transfer experiments now are in agreement, the low-energy S factor underpredicts the low-energy reaction data by a considerable amount. While the S factor of La Cognata *et al.* [31] has been revised to a lower value (see Sec. VI), the original calculation is in much better agreement with the $^{13}C(\alpha,n)^{16}O$ data and therefore serves as an estimate of the extrapolation of the data of Drotleff *et al.* [8] and Heil *et al.* [9], as shown in Fig. 8.

IX. SUMMARY OF UNCERTAINTY CONTRIBUTIONS

The above calculations of the different uncertainty contributions to the low-energy $^{13}C(\alpha,n)^{16}O$ S factor have found that the uncertainty stems from three main sources: the uncertainty in $\widetilde{C}^2$ of the near-threshold state (20%), the inconsistency between the energy dependence of the low-energy $^{13}C(\alpha,n)^{16}O$ data and the R-matrix fits constrained by $\widetilde{C}^2$ (40%), and the overall normalization uncertainty of the $^{13}C(\alpha,n)^{16}O$ data (16%).

On the other hand, it has been found that the uncertainty in the level energy of the near-threshold state, at least to ± 8 keV, does not contribute significantly to the uncertainty in the S factor (5%). In addition, taking the results of Keeley *et al.* [29], for the dependence of the DWBA fit on the energy of the near-threshold level, the effect is found to be about 10%, which is not significant at this time. The uncertainty in Γ_n is also found to be on the 5% level and therefore can currently be neglected. Additionally, the uncertainties in the masses and Q values of the reaction are also negligible. Coming back to the recent measurement of Faestermann *et al.* [32] of the energy and width of the near-threshold state, these results will not affect the uncertainty in the extrapolation of the $^{13}C(\alpha,n)^{16}O$ S factor until the much larger uncertainty sources above are reduced.

X. UNCERTAINTY IN THE REACTION RATE

The significant sources of uncertainties in the $^{13}C(\alpha,n)^{16}O$ cross section summarized in Sec. IX are now used to calculate the uncertainty in the reaction rate over the astrophysical temperature range of interest. Taking the upper uncertainty of La Cognata *et al.* [31] to represent the upper uncertainty from the reaction data and the lower uncertainty of Avila *et al.* [33] to represent the lower uncertainty from $\widetilde{C}^2$ measurements, results in an uncertainty in the reaction rate at low temperatures from 0.1 to 0.3 GK of 40% to 10%, respectively. This encapsulates both the uncertainty in $\widetilde{C}^2$ and the inconsistency between the R-matrix cross section calculated with the value of $\widetilde{C}^2$ from Avila *et al.* [33] and the $^{13}C(\alpha,n)^{16}O$ cross-section data. The absolute normalization of the $^{13}C(\alpha,n)^{16}O$ cross section translates directly to the

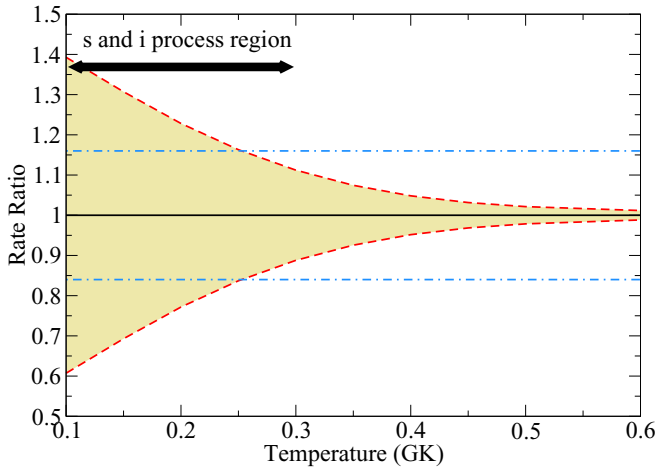

FIG. 9. Uncertainty in the rate stemming from the uncertainty and inconsistency between the values of $\widetilde{C}^2$ for the near-threshold state reported by Avila *et al.* [33] and La Cognata *et al.* [31] as a function of temperature for the $^{13}C(\alpha,n)^{16}O$ reaction. The blue dotted-dashed line represents the discrepancy on the scale of the evaluated cross section between the recent evaluations [49,51].

uncertainty on the reaction rate, which has been treated here simply as a constant uncertainty of ±16%. Figure 9 shows the relative contributions.

In addition, it is useful to examine the contribution that the near-threshold state makes to the reaction rate depending on these upper and lower rate limits. The low-energy S factor has been calculated with no contribution from the near-threshold resonance as shown by the dashed gray line in Fig. 8. The fraction of the reaction rates from the $\widetilde{C}^2$ values of La Cognata *et al.* [31] and Avila *et al.* [33] are then divided by the rate where no near-threshold state is included, as shown in Fig. 10. This highlights the importance of the near-threshold state at low temperatures and also demonstrates that it quickly becomes a small contribution above ≈0.4 GK.

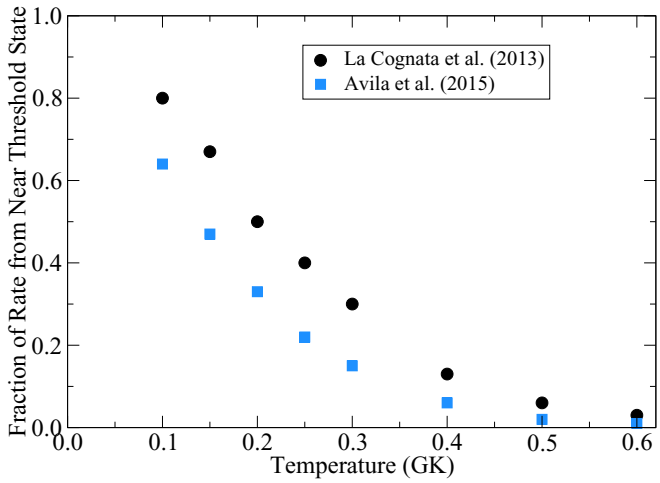

FIG. 10. Fraction of the reaction rate stemming from the high-energy tail of the near-threshold state as a function of temperature. The black circles indicate the calculation using the central value of the S factor determined by using the $\widetilde{C}^2$ of La Cognata *et al.* [31] while the blue squares correspond to that of Avila *et al.* [33].

XI. SUMMARY

The sensitivity in the rate of the $^{13}C(\alpha,n)^{16}O$ reaction to the uncertainties in the level parameters of the near-threshold state at $E_x = 6.356$ MeV in ^{17}O have been investigated over the temperature region important for s- and i-process nucleosynthesis. Recently, Keeley *et al.* [29] demonstrated that performing the DWBA analysis at different energies gives a rather broad spread of $\widetilde{C}^2$. It has been shown that this variation propagates to ≈10% uncertainty in the low-energy $^{13}C(\alpha,n)^{16}O$ S factor. Reviewing the most precisely quoted values for $\widetilde{C}^2$ and propagating those uncertainties to the S factor gives an uncertainty of 20%, but inconsistencies between the energy dependence of the S factor for the low-energy $^{13}C(\alpha,n)^{16}O$ experimental data and those calculated based on $\widetilde{C}^2$ gives a range of values that vary by ≈40%. The affect of the uncertainty in the neutron width of the near-threshold state on the S factor has also been investigated, and it is found to be at the 5% uncertainty level or smaller. Finally, the inconsistency in the overall normalization of the $^{13}C(\alpha,n)^{16}O$ experimental data remains a significant source of uncertainty.

Based on these results, experimental investigations of the energy dependence of the low-energy $^{13}C(\alpha,n)^{16}O$ cross section are highly desired. Past measurements over the very-low-energy region have large uncertainties due to low count rates and a large background component to the experimental yields. New measurements at high beam intensity, low background, underground facilities are thus of high priority. Of nearly equal importance are new measurements dedicated to solving the discrepancy between the absolute normalization of the $^{13}C(\alpha,n)^{16}O$ cross-section data. These experiments will likely involve novel experimental techniques to achieve a low uncertainty in the neutron detection efficiency and require systematic studies of different target types in order to more accurately determine the number of active target nuclei.

Finally, while the recent analysis of Leal *et al.* [5] and that found in ENDF/B-VIII.0 [49] are very comprehensive, an updated R-matrix analysis that focuses on the low-energy $^{13}C(\alpha,n)^{16}O$ cross section and extrapolation is needed. The last analysis of this kind by Heil *et al.* [9] included more than 37 000 data points and 74 levels (plus 10 background levels) covering the majority of the available $^{13}C+\alpha$ and $^{16}O+n$ data sets available at that time. An updated analysis should include all of this previous data and also take into account the results of the new measurements, in particular those that have provided new information on the properties of the near-threshold state. This is a major undertaking and emphasizes the need for further documentation and reproducibility of these types of large-scale R-matrix projects with publicly available and benchmarked codes [53].

ACKNOWLEDGMENTS

This research utilized resources from the Notre Dame Center for Research Computing. This work was also facilitated by a series of Consultant Meetings on "R-matrix

Codes for Charged-particle reactions in the resolved resonance region" by the International Atomic Energy Agency. R.J.D., J.G., and M.W. were supported by the National Science Foundation through Grant No. Phys-1713857, and the Joint Institute for Nuclear Astrophysics through Grants No. Phys-0822648 and No. PHY-1430152 (JINA Center for the Evolution of the Elements). C.R.B. acknowledges support from U.S. D.O.E. through Grants No. DE-FG02-88ER40387 and No. DE-NA0003883, and the work of I.J.T. was performed under the auspices of the U.S. Department of Energy by Lawrence Livermore National Laboratory under Contract DE-AC52-07NA27344.

[1] S. Bisterzo, C. Travaglio, M. Wiescher, F. Käppeler, and R. Gallino, Astrophys. J. Lett. **835**, 97 (2017).
[2] S. Jones, C. Ritter, F. Herwig, C. Fryer, M. Pignatari, M. G. Bertolli, and B. Paxton, Mon. Not. R. Astron. Soc. **455**, 3848 (2015).
[3] S. Cristallo, M. L. Cognata, C. Massimi, A. Best, S. Palmerini, O. Straniero, O. Trippella, M. Busso, G. F. Ciani, F. Mingrone, L. Piersanti, and D. Vescovi, Astrophys. J. Lett. **859**, 105 (2018).
[4] S. Bisterzo, C. Travaglio, R. Gallino, M. Wiescher, and F. Käppeler, Astrophys. J. **787**, 10 (2014).
[5] L. Leal, E. Ivanov, G. Noguere, A. Plompen, and S. Kopecky, EPJ Nucl. Sci. Technol. **2**, 43 (2016).
[6] S. Chakraborty, R. deBoer, A. Mukherjee, and S. Roy, Phys. Rev. C **91**, 045801 (2015).
[7] C. N. Davids, Nucl. Phys. A **110**, 619 (1968).
[8] H. W. Drotleff, A. Denker, H. Knee, M. Soine, G. Wolf, J. W. Hammer, U. Greife, C. Rolfs, and H. P. Trautvetter, Astrophys. J. **414**, 735 (1993).
[9] M. Heil, R. Detwiler, R. E. Azuma, A. Couture, J. Daly, J. Görres, F. Käppeler, R. Reifarth, P. Tischhauser, C. Ugalde, and M. Wiescher, Phys. Rev. C **78**, 025803 (2008).
[10] S. Harissopulos, H. W. Becker, J. W. Hammer, A. Lagoyannis, C. Rolfs, and F. Strieder, Phys. Rev. C **72**, 062801(R) (2005).
[11] E. Ramström and T. Wiedling, Nucl. Phys. A **272**, 259 (1976).
[12] C. R. Brune, I. Licot, and R. W. Kavanagh, Phys. Rev. C **48**, 3119 (1993).
[13] S. Kellogg, R. Vogelaar, and R. Kavanagh, Bull. Amer. Phys. Soc. **34**, 1192 (1989).
[14] D. Tilley, H. Weller, and C. Cheves, Nucl. Phys. A **564**, 1 (1993).
[15] W. Huang, G. Audi, M. Wang, F. Kondev, S. Naimi, and X. Xu, Chin. Phys. C **41**, 030002 (2017).
[16] M. Wang, G. Audi, F. Kondev, W. Huang, S. Naimi, and X. Xu, Chin. Phys. C **41**, 030003 (2017).
[17] M. Wiescher and T. Ahn, *Nuclear Particle Correlations and Cluster Physics* (World Scientific, Singapore, 2017), Chap. 8, pp. 203–255.
[18] K. Ikeda, T. Marumori, R. Tamagaki, and H. Tanaka, Prog. Theor. Phys. Suppl. **52**, 1 (1972).
[19] P. Descouvemont, Phys. Rev. C **36**, 2206 (1987).
[20] J. Okołowicz, M. Płoszajczak, and W. Nazarewicz, Prog. Theor. Phys. Suppl. **196**, 230 (2012).
[21] J. Okołowicz, W. Nazarewicz, and M. Płoszajczak, Fortschr. Phys. **61**, 66 (2013).
[22] L. Blokhintsev, I. Borbély, and É. I. Dolinskiĭ, Fiz. Élem. Chastis At. Yadra **8**, 1189 (1977) [Sov. J. Part. Nucl. **8**, 485 (1977)].
[23] R. E. Tribble, C. A. Bertulani, M. L. Cognata, A. M. Mukhamedzhanov, and C. Spitaleri, Rep. Prog. Phys. **77**, 106901 (2014).
[24] R. Yarmukhamedov and L. Blokhintsev, Phys. At. Nucl. **81**, 616 (2018).
[25] A. M. Mukhamedzhanov, C. A. Gagliardi, and R. E. Tribble, Phys. Rev. C **63**, 024612 (2001).
[26] A. M. Lane and R. G. Thomas, Rev. Mod. Phys. **30**, 257 (1958).
[27] A. M. Mukhamedzhanov and R. E. Tribble, Phys. Rev. C **59**, 3418 (1999).
[28] A. M. Mukhamedzhanov, Phys. Rev. C **86**, 044615 (2012).
[29] N. Keeley, K. W. Kemper, and K. Rusek, Eur. Phys. J. A **54**, 71 (2018).
[30] R. Sayer, L. Leal, N. Larson, R. Spencer, and R. Wright, J. Nucl. Sci. Technol. (Abingdon, U. K.) **39**, 88 (2002).
[31] M. La Cognata, C. Spitaleri, O. Trippella, G. G. Kiss, G. V. Rogachev, A. M. Mukhamedzhanov, M. Avila, G. L. Guardo, E. Koshchiy, A. Kuchera *et al.*, Astrophys. J. **777**, 143 (2013).
[32] T. Faestermann, P. Mohr, R. Hertenberger, and H.-F. Wirth, Phys. Rev. C **92**, 052802(R) (2015).
[33] M. L. Avila, G. V. Rogachev, E. Koshchiy, L. T. Baby, J. Belarge, K. W. Kemper, A. N. Kuchera, and D. Santiago-Gonzalez, Phys. Rev. C **91**, 048801 (2015).
[34] A. M. Mukhamedzhanov, Shubhchintak, and C. A. Bertulani, Phys. Rev. C **96**, 024623 (2017).
[35] O. Trippella and M. La Cognata, Astrophys. J. Lett. **837**, 41 (2017).
[36] R. E. Azuma, E. Uberseder, E. C. Simpson, C. R. Brune, H. Costantini, R. J. de Boer, J. Görres, M. Heil, P. J. LeBlanc, C. Ugalde, and M. Wiescher, Phys. Rev. C **81**, 045805 (2010).
[37] E. Uberseder and R. J. deBoer, *AZUER2 User Manual* (2015).
[38] C. R. Brune, Phys. Rev. C **66**, 044611 (2002).
[39] See Supplemental Material at http://link.aps.org/supplemental/10.1103/PhysRevC.101.045802 for ^{13}C+a.azr input file.
[40] R. J. deBoer, J. Görres, M. Wiescher, R. E. Azuma, A. Best, C. R. Brune, C. E. Fields, S. Jones, M. Pignatari, D. Sayre, K. Smith, F. X. Timmes, and E. Uberseder, Rev. Mod. Phys. **89**, 035007 (2017).
[41] M. La Cognata, C. Spitaleri, O. Trippella, G. G. Kiss, G. V. Rogachev, A. M. Mukhamedzhanov, M. Avila, G. L. Guardo, E. Koshchiy, A. Kuchera *et al.*, Phys. Rev. Lett. **109**, 232701 (2012).
[42] S. Y. Mezhevych, A. T. Rudchik, A. A. Rudchik, O. A. Ponkratenko, N. Keeley, K. W. Kemper, M. Mazzocco, K. Rusek, and S. B. Sakuta, Phys. Rev. C **95**, 034607 (2017).
[43] M. G. Pellegriti, F. Hammache, P. Roussel, L. Audouin, D. Beaumel, P. Descouvemont, S. Fortier, L. Gaudefroy, J. Kiener, A. Lefebvre-Schuhl, M. Stanoiu *et al.*, Phys. Rev. C **77**, 042801(R) (2008).
[44] B. Guo, Z. H. Li, M. Lugaro, J. Buntain, D. Y. Pang, Y. J. Li, J. Su, S. Q. Yan, X. X. Bai, Y. S. Chen *et al.*, Astrophys. J. **756**, 193 (2012).

[45] J. L. Fowler, C. H. Johnson, and R. M. Feezel, Phys. Rev. C **8**, 545 (1973).

[46] S. Cierjacks, P. Forti, D. Kopsch, L. Kropp, J. Nebe, and H. Unseld, *High Resolution Total Neutron Cross Sections Between 0.5 and 30 MeV*, Tech. Rep. (Karlsruhe Institute of Technology, Germany, 1968), KFK-1000 (unpublished).

[47] D. Larson, J. Harvey, and N. Hill, in *Proc. Int. Conf. On Nuclear Cross Sections for Technology, Knoxville* (1980), p. 34.

[48] D. Larson, in *Symposium on Neutron Cross Section from 10 to 50 MeV, BNL-NCS-51245* (1980), p. 277.

[49] D. Brown, M. Chadwick, R. Capote, A. Kahler, A. Trkov, M. Herman, A. Sonzogni, Y. Danon, A. Carlson, M. Dunn *et al.*, Nucl. Data Sheets **148**, 1 (2018).

[50] M. Chadwick, R. Capote, A. Trkov, M. Herman, D. Brown, G. Hale, A. Kahler, P. Talou, A. Plompen, P. Schillebeeckx *et al.*, Nucl. Data Sheets **148**, 189 (2018).

[51] M. Chadwick, M. Herman, P. Obložinský, M. Dunn, Y. Danon, A. Kahler, D. Smith, B. Pritychenko, G. Arbanas, R. Arcilla *et al.*, Nucl. Data Sheets **112**, 2887 (2011).

[52] J. K. Bair and F. X. Haas, Phys. Rev. C **7**, 1356 (1973).

[53] I. J. Thompson, R. J. deBoer, P. Dimitriou, S. Kunieda, M. T. Pigni, G. Arbanas, H. Leeb, T. Srdinko, G. Hale, P. Tamagno, and P. Archier, Eur. Phys. J. A **55**, 92 (2019).